Contribution from the Institut für Physikalische und Theoretische Chemie, University of Erlangen-Nürnberg, D-8520 Erlangen, West Germany, Institut für Heisse Chemie, Kernforschungszentrum Karlsruhe, D-7500 Karlsruhe, West Germany, and Department of Chemistry, The University of New South Wales, Kensington, NSW 2033, Australia

Detailed Study of the Hysteresis Associated with the Spin-State Transition in Bis(2,6-bis(pyrazol-3-yl)pyridine)iron(II) Bis(tetrafluoroborate) and the Hypothesis of Independent Domains

E. König,*[1] B. Kanellakopulos,[2] B. Powietzka,[2] and H. A. Goodwin[3]

Received May 3, 1989

An extensive series of scanning curves within the hysteresis loop associated with the spin-state transition in $[Fe(bpp)_2](BF_4)_2$ has been constructed on the basis of magnetic susceptibility measurements (bpp = 2,6-bis(pyrazol-3-yl)pyridine). The areas of the scanning curves are found to depend on the actual temperature range encompassed by the curves and on the value of the square of the effective magnetic moment defined at the center of gravity of the curves. The results do not conform to theorem 4 of the domain theory of Everett, and the implications of these findings for the nature of first-order spin-state transitions are discussed.

Spin-state transitions in complexes of certain transition-metal ions often are associated with pronounced hysteresis effects. It has been pointed out[4] that the observed hysteresis is indicative of the first-order nature of the transition, since such a transition always requires some degree of superheating or supercooling for kinetic reasons. Additional evidence for a thermodynamically first-order transition is provided by the sizable latent heat and associated discontinuous change of entropy[5-8] as well as by the change of volume derived on the basis of X-ray diffraction measurements[9] or the second-order Doppler shift of the Mössbauer effect.[10,11] Thermal hysteresis of the kind observed may have its origin in either (i) a distribution of transition temperatures as the result of domain formation or (ii) a distribution of nucleation rates as a consequence of kinetic barriers. A detailed study of the hysteresis effects can be helpful in establishing the nature of the cooperativity of the transition. Thus, the model developed by Everett[12-14] has been applied to study domain formation, whereas VWBD theory[15,16] should govern nucleation rates.

In the Everett model, theorem 4, which relates to the areas of inner loops of hysteresis ("scanning curves"), is particularly diagnostic. According to this theorem, form and area of two scanning curves, constructed between the same temperature limits T_A and T_B, should be equal,[13] *provided that the domains are independent*.[17]

In the first detailed study of scanning curves of the hysteresis associated with a spin-state transition, two such curves were constructed for the system $[Fe(phy)_2](ClO_4)_2$ on the basis of X-ray powder diffraction measurements (phy = 1,10-phenanthroline-2-carbaldehyde phenylhydrazone).[18] It was found that the areas bound by the two curves were equal to within 3%. Hence, it was concluded that the course of the transition is accompanied by the formation of *independent* domains. In a subsequent study, Müller et al.[19] investigated scanning curves of the hysteresis associated with the spin-state transition in $[Fe(bt)_2(NCS)_2]$ on the basis of magnetic susceptibility measurements (bt = 2,2'-bi-2-thiazoline). These authors obtained an agreement of 4 ± 1% for the areas of two scanning curves and also concluded on this basis that independent domains were involved in the transition.

In the present paper, we report the results of an extended study of the hysteresis associated with the spin-state transition in $[Fe(bpp)_2](BF_4)_2$, where bpp = 2,6-bis(pyrazol-3-yl)pyridine. The study was undertaken in order to test the general validity of the earlier results[18,19] obtained for $[Fe(phy)_2](ClO_4)_2$ and $[Fe(bt)_2(NCS)_2]$. For this purpose, multiple scanning curves of all three types, i.e. left boundary, entire inner, and right boundary, were obtained for the first time. The compound was chosen because its reasonably wide hysteresis at the transition is particularly well suited for the present study. Thus, the transition temperatures have been reported[20] as $T_c^{\uparrow}$ = 183 K and $T_c^{\downarrow}$ = 173 K. All the results were derived on the basis of very accurate magnetic susceptibility measurements.

Table I. Results of Magnetic Susceptibility Measurements on Scanning Curve No. 4 within the Hysteresis Loop at the Spin-State Transition in $[Fe(bpp)_2](BF_4)_2$

pt no.	T, K	χ_M,[a] cgsu mol^{-1}	μ_{eff}^2, μ_B^2	μ_{eff},[b] μ_B
1	174.0	15282	21.27	4.612
2	175.1	15156	21.23	4.608
3	176.1	15109	21.29	4.614
4	177.1	15111	21.41	4.627
5	178.5	15099	21.56	4.643
6	179.65	15158	21.79	4.668
7	180.5	15341	22.15	4.706
8	179.45	15383	22.08	4.699
9	178.6	15409	22.02	4.692
10	177.4	15414	21.88	4.677
11	176.25	15411	21.74	4.663
12	175.2	15338	21.49	4.636
13	174.25	15245	21.25	4.610
14	174.0	15198	21.16	4.600

[a] Experimental uncertainty ±20 × 10^{-6} cgsu mol^{-1}. [b] Experimental uncertainty ±0.005 μ_B.

Experimental Section

Sample Preparation. The ligand was prepared by the method reported by Lin and Lang,[21] and the complex $[Fe(bpp)_2](BF_4)_2$ was obtained by interaction of the ligand with iron(II) tetrafluoroborate in hot ethanolic

(1) University of Erlangen-Nürnberg.
(2) Kernforschungszentrum Karlsruhe.
(3) University of New South Wales.
(4) König, E.; Ritter, G.; Kulshreshtha, S. K. *Chem. Rev.* **1985**, *85*, 219.
(5) Sorai, M.; Seki, S. *J. Phys. Chem. Solids* **1974**, *35*, 555.
(6) Kulshreshtha, S. K.; Iyer, R. M.; König, E.; Ritter, G. *Chem. Phys. Lett.* **1984**, *110*, 201.
(7) Kulshreshtha, S. K.; Sasikala, R.; König, E. *Chem. Phys. Lett.* **1986**, *123*, 215.
(8) Kulshreshtha, S. K.; Iyer, R. M. *Chem. Phys. Lett.* **1987**, *134*, 239.
(9) König, E. *Prog. Inorg. Chem.* **1987**, *35*, 527.
(10) König, E.; Ritter, G.; Kulshreshtha, S. K.; Nelson, S. M. *J. Am. Chem. Soc.* **1983**, 105, 1924.
(11) König, E.; Ritter, G.; Kulshreshtha, S. K.; Goodwin, H. A. *Inorg. Chem.* **1983**, *22*, 2518.
(12) Everett, D. H.; Whitton, W. I. *Trans. Faraday Soc.* **1952**, *48*, 749.
(13) Everett, D. H.; Smith, F. W. *Trans. Faraday Soc.* **1954**, *50*, 187.
(14) Everett, D. H. *Trans. Faraday Soc.* **1954**, *50*, 1077; **1955**, *51*, 1551.
(15) Volmer, M.; Weber, A. *Z. Phys. Chem.* **1925**, *119*, 277.
(16) Becker, R.; Döhring, W. *Ann. Phys.* **1935**, *24*, 719.
(17) Enderby, A. *Trans. Faraday Soc.* **1955**, *52*, 106.
(18) König, E.; Ritter, G.; Irler, W.; Goodwin, H. A. *J. Am. Chem. Soc.* **1980**, *102*, 4681.
(19) Müller, E. W.; Spiering, H.; Gütlich, P. *J. Chem. Phys.* **1983**, *79*, 1439.
(20) Goodwin, H. A.; Sugiyarto, K. H. *Chem. Phys. Lett.* **1987**, *139*, 470.
(21) Lin, Y.-i; Lang, S. A. *J. Heterocycl. Chem.* **1977**, *14*, 345.

0020-1669/89/1328-3993$01.50/0 © 1989 American Chemical Society

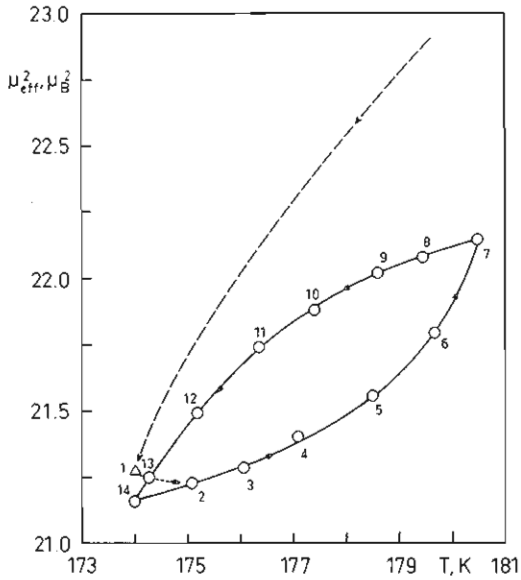

Figure 1. Scanning curve no. 4 within the hysteresis loop at the spin-state transition in $[Fe(bpp)_2](BF_4)_2$. Individual data points are numbered according to the order of measurement.

solution.[20] The resulting complex is hydrated, the anhydrous form employed in this study being obtained by heating the hydrated complex at 110 °C in a nitrogen atmosphere. The purity of the sample was checked by elemental analyses for C, H, N, and Fe and by ^{57}Fe Mössbauer spectroscopy.

Magnetic Measurements. Magnetic susceptibilities were measured with a Faraday type magnetometer equipped with a custom-made helium/N_2 bath cryostat. The magnetometer employs a 10 in. B-E25C8 electromagnet (Bruker-Physik) with Henry type pole caps, an electrical microbalance (Sartorius type 4102), and the required control electronics. Measurement and regulation of sample temperature is achieved by two independent Cu/constantan and Au(Fe)/chromel thermocouples calibrated against a Pt or Ge resistor. The calibration was carefully checked against the inverse magnetic susceptibility of three standard substances that are known to follow rigorously the Curie–Weiss law below 10 K, viz. $FeSO_4 \cdot 7H_2O$, $CuSO_4 \cdot 5H_2O$, and $K_2Ni(SO_4)_2 \cdot 6H_2O$.[22] Using this procedure, we achieved an absolute accuracy of temperature determination of ±0.02 K between 0.98 and 9.0 K. This calibration was subsequently extended to higher temperatures, thus implicitly assuming validity of the linear $1/\chi_M$ vs T relationship. This assumption was further corroborated by measurements of numerous standard substances over an extended period of time. $HgCo(NCS)_4$, $Ni(en)_2S_2O_3$, and $CuSO_4 \cdot 5H_2O$ were used as susceptibility standards.[23] The effective magnetic moment has been obtained according to $\mu_{eff} = 2.828\ (\chi_M^{cor} T)^{1/2}$, where χ_M^{cor} is the molar magnetic susceptibility corrected for diamagnetism of all constituents and T the temperature in K.

In order to demonstrate the reliability and accuracy of data on which the present study is based, Figure 1 shows, in terms of μ_{eff}^2 values, a single scanning curve within the hysteresis loop of $[Fe(bpp)_2](BF_4)_2$, the corresponding experimental data being collected in Table I. The curve is in fact inner scanning curve no. 4 (for the notation, refer to Table II) between the temperatures T_A = 174.0 K and T_B = 180.5 K (μ_{eff}^2 = 21.16 and 22.15 μ_B^2, respectively). The individual data points are numbered consecutively following the order of measurement. Point 1 has been obtained by cooling of the sample from the higher temperature of 184.8 K where μ_{eff}^2 = 26.31 μ_B^2. The difference of μ_{eff}^2 values between the initial and final points 1 and 14 at T_A, i.e. 21.27 and 21.16 μ_B^2, respectively, corresponds to 0.52% and is caused by a slight imbalance of temperature. Evidently, the relative accuracy of the results is considerably higher.

Results

According to measurements of magnetic susceptibility the spin-state transition in the actual sample of $[Fe(bpp)_2](BF_4)_2$ studied in this work is at $T_c^{\uparrow}$ = 181.9 K for increasing and at $T_c^{\downarrow}$ = 171.5 K for decreasing temperatures, thus producing an hysteresis loop of width ΔT_c = 10.4 K. Inner scanning curves of width ΔT = 6.5 K have been measured between the same two temperatures T_A = 174.0 K and T_B = 180.5 K (curves 1–4). The detailed procedure for this type of measurement has been given by Everett and Smith.[13] In addition, scanning curves contacting the right-boundary curve of the hysteresis loop ("right-boundary

Table II. Characteristic Properties of Scanning Curves of Hysteresis at the Spin-State Transition in $[Fe(bpp)_2](BF_4)_2$

no.	temp, K[a] T_A	T_B	ΔT	μ_{eff}^2, μ_B^2 at T_A	at T_B	area[b]	character of curve
Ξ	170.5	181.7	11.2	6.04	15.45	108.4	
1	174.0	180.5	6.5	8.25	10.34	9.73	inner sc
2				13.99	15.63	7.82	
3				18.74	19.99	6.47	
4				21.16	22.15	4.26	
I ≡ 1	174.0	180.5	6.5	8.25	10.34	9.73	right-boundary sc
II	175.0	181.5	6.5	11.67	13.81	10.61	
III	176.5	183.0	6.5	20.12	21.18	4.83	
α	170.0	176.5	6.5	9.60	10.59	2.37	left-boundary sc
β	171.7	178.2	6.5	15.38	16.37	2.91	
γ	172.6	179.1	6.5	19.58	20.48	3.11	
δ	173.4	179.9	6.5	24.20	24.84	1.90	
A	173.0	176.0	3.0	4.25	4.58	0.23	right-boundary sc
B	175.5	178.5	3.0	5.79	6.28	0.50	
C	177.2	180.2	3.0	9.14	9.75	0.85	
D	178.5	181.5	3.0	12.68	13.24	0.74	
a ≡ A	173.0	176.0	3.0	4.25	4.58	0.23	inner sc
b				5.88	6.25	0.27	
c				7.42	7.77	0.33	
d				8.70	9.03	0.27	
e				11.11	11.43	0.22	
f				12.05	12.33	0.22	
g				13.69	13.95	0.16	

[a] $T_A - T_B$ is the range of temperatures covered by the particular scanning curve. [b] Area $\mu_{eff}^2 T$ in units of μ_B^2 K.

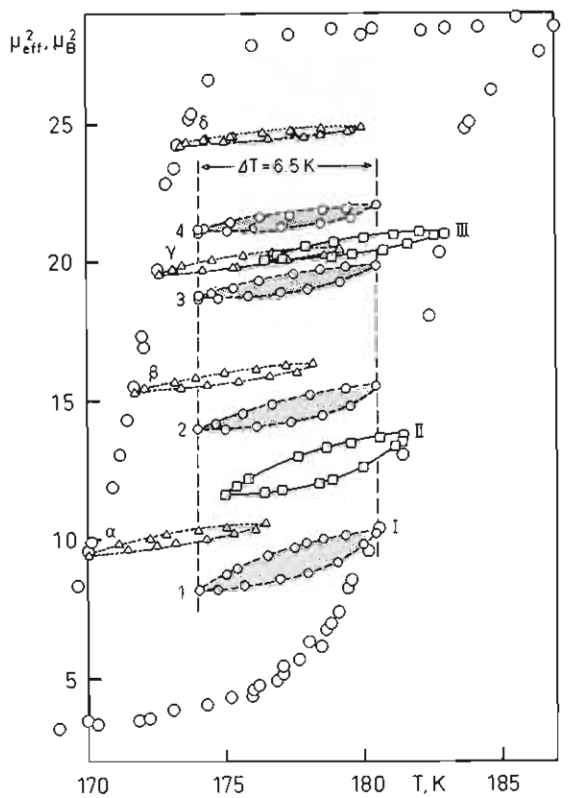

Figure 2. Inner scanning curves of width ΔT = 6.5 K between the temperatures T_A = 174.0 K and T_B = 180.5 K (curves 1–4, hatched) within the hysteresis loop at the spin-state transition in $[Fe(bpp)_2](BF_4)_2$. Right-boundary scanning curves (curves I–III) and left-boundary scanning curves (curves α–δ) of width ΔT = 6.5 K between different initial temperatures T_A and final temperatures T_B are also shown.

(22) Aderhold, C.; Baumgärtner, F.; Dornberger, E.; Kanellakopulos, B. *Z. Naturforsch.* **1978**, *33A*, 1268.
(23) Figgis, B. N.; Lewis, J. In Technique of Inorganic Chemistry; Jonassen, H. B., Weissberger, A., Eds.; Interscience: New York, 1965, Vol. 4.

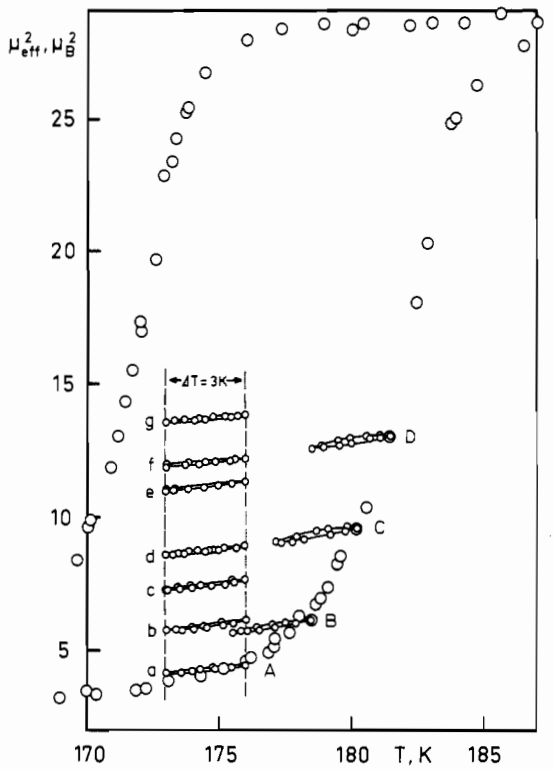

Figure 3. Inner scanning curves of width ΔT = 3.0 K between the temperatures T_A = 173.0 K and T_B = 176.0 K (curves a–g) within the hysteresis loop at the spin-state transition in $[Fe(bpp)_2](BF_4)_2$. Right-boundary scanning curves of width ΔT = 3.0 K between different initial temperatures T_A and final temperatures T_B (curves A–D) are also shown.

scanning curves") with ΔT = 6.5 K but different initial temperatures T_A and final temperatures T_B (curves I–III) have been constructed. A similar series of curves contacting the left-boundary curve ("left-boundary scanning curves") with ΔT = 6.5 K (curves α–δ) have also been obtained. These curves are displayed in Figure 2. Furthermore, scanning curves of width ΔT = 3.0 K have been measured both as inner scanning curves for T_A = 173.0 K and T_B = 176.0 K (curves a–g) and as right-boundary scanning curves (curves A–D). These curves are shown in Figure 3. The individual curves are identified, in the figures, by a specific label, their characteristic properties being listed under the same label in Table II. The curve designated by Ξ in the table is a single large scanning curve, which has not been reproduced in any of the figures in detail. In Figure 4, the reduced area F/F_{tot} of the scanning curves is plotted as a function of the effective magnetic moment squared of the particular scanning curve. A logarithmic scale has been used, the quantity F_{tot} being the area of the overall hysteresis loop. Each scanning curve is thus represented by a bar that extends over the range of μ_{eff}^2 values covered by that curve. It is seen that the individual scanning curves order on a curve of approximately parabolic shape for each specific value of the temperature range ΔT covered. The bars representing the inner scanning curves and those representing the left-boundary scanning curves order below the curve for the right-boundary scanning curve. It should be observed that the parabolic curves exist only within the boundaries of the hysteresis loop. In addition, the F/F_{tot} curve representing the inner scanning curves exists only within the interval defined by contact with the parabolas of right- and left-boundary scanning curves.

Discussion

According to theorem 4 in the Everett model, the areas of the inner scanning curves 1–4 (Figure 2), all measured between the same temperatures T_A = 174.0 and T_B = 180.5 K, should be equal if the model applies to this system. Similarly, the inner scanning curves a–g (Figure 3) between T_A = 173.0 and T_B v 176.0 K should all be of equal area. It is obvious from the figures that this is not the case, and the differences in area are particularly evident for the curves 1–4. For this series, the area difference

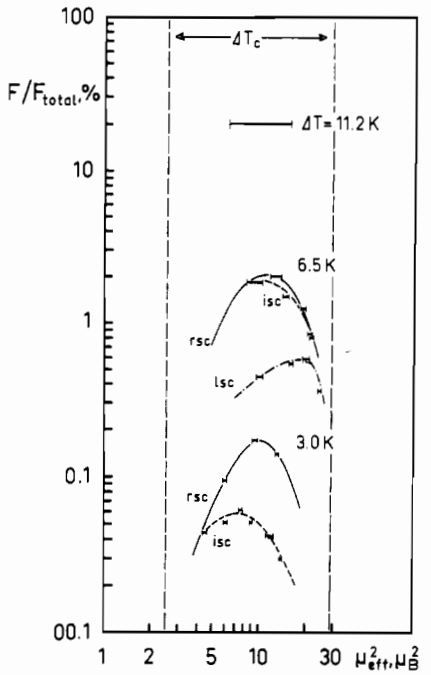

Figure 4. Reduced area of scanning curves F/F_{tot} (in percent) as a function of the effective magnetic moment squared μ_{eff}^2 (in μ_B^2) for the spin-state transition in $[Fe(bpp)_2](BF_4)_2$ on double logarithmic scale. F_{tot} denotes the area of the overall hysteresis loop. Bars indicate range of μ_{eff}^2 values covered by a particular curve; rsc = right-boundary scanning curve, isc = inner scanning curve, and lsc = left-boundary scanning curve. Curves order according to the ΔT values 6.5 and 3.0 K.

for adjacent curves amounts to 1.91 μ_B^2 K or 19.6% for curves 1 and 2, to 1.35 μ_B^2 K or 17.3% for curves 2 and 3, and to 2.21 μ_B^2 K or 34.2% for curves 3 and 4. A more detailed inspection of the areas listed in Table II shows that, for each series of inner scanning curves, the values pass over a maximum. The areas of the left- or right-boundary scanning curves are different from those of the inner scanning curves, as expected, but, significantly, they also display, for a particular ΔT range, a similar behavior. This result is illustrated by Figure 4, which shows that the areas are distributed on a curve of approximately parabolic shape for each particular value of ΔT. The range of existence of these curves is determined by the μ_{eff}^2 values covered by the boundary hysteresis curve of the compound, which is indicated in Figure 4 by the broken vertical lines defined by the limiting μ_{eff}^2 values of about 2.5 and 30 μ_B^2.

These results are clearly not consistent with theorem 4 of the domain theory of Everett.[13] According to this theorem, the areas of inner scanning curves would have to order, in terms of the presentation of Figure 4, along the horizontal line defining a particular value of the relative area, and this they do not do. It has been pointed out that the theorem is applicable only to the case of independent domains.[17] The present results could thus still be interpreted by assuming that the spin-state transition in $[Fe(bpp)_2](BF_4)_2$ occurs by the coonversion of domains of like spin. The domains would, however, have to show interaction with each other. This conclusion is in no way surprising, since interaction at least between different molecules of a spin-crossover compound is required in several theoretical models of these transitions. The interaction may be limited to HS ions as in the simplified version of an Ising type model[24] or comprise the interactions between two HS ions, between a HS and a LS ion, and between two LS ions.[25] In the more general Ising type model, domain formation by both HS and LS molecules would be expected.

In view of the rather large differences in areas of 34% and more that are observed for the present compound, it is surprising that the areas of scanning curves reported for $[Fe(phy)_2](ClO_4)_2$ and

(24) Zimmermann, R.; König, E. *J. Phys. Chem. Solids* **1977**, *38*, 779.
(25) Rao, P. S.; Ganguli, P.; McGarvey, B. R. *Inorg. Chem.* **1981**, *20*, 3682.

$[Fe(bt)_2(NCS)_2]$ were found to be equal within 3% and 4%, respectively.[18,19] It is conceivable that the spin-state transitions in these systems may take place by the formation of independent domains whereas interacting domains appear to be present in $[Fe(bpp)_2](BF_4)_2$ (and may occur in other systems). The conditions defining this difference in behavior would, nevertheless, still need to be specified.

The difference may be illusory rather than real, however. The nature of the distribution of areas shown in Figure 4 may provide an alternative explanation for the apparent difference in the behavior of $[Fe(phy)_2](ClO_4)_2$ and $[Fe(bt)_2(NCS)_2]$ on the one hand and $[Fe(bpp)_2](BF_4)_2$ on the other. Thus, scanning curves situated close to the maximum of one of the parabolic curves, or being disposed symmetrically with respect to that maximum, will have similar (but not identical) areas, whereas the areas of scanning curves located on the slope of one of the parabolas will be significantly different. The observation of almost equal areas could thus be fortuitous and the result of the range of μ_{eff}^2 chosen for study. The applicability of the independent domain model is thus not necessarily established by the behavior of only a small number of scanning curves. A more detailed study of the hysteresis by construction of an extended series of curves within the same temperature limits is required to determine if the behavior of $[Fe(phy)_2](ClO_4)_2$ and $[Fe(bt)_2(NCS_2)]$ is in fact different from that of $[Fe(bpp)_2](BF_4)_2$, and work along these lines is currently in progress in our laboratories.

Acknowledgment. We appreciate financial support by the Deutsche Forschungsgemeinschaft, Bonn, West Germany.

Registry No. $[Fe(bpp)_2](BF_4)_2$, 111994-63-9.

Contribution from the Chemistry Department, University of Tasmania, Box 252C, Hobart, Tasmania 7001, Australia

Electronic, EPR, and Vibrational Spectra of the $CuCl_6^{4-}$ Ion

Robbie G. McDonald and Michael A. Hitchman*

Received February 14, 1989

The electronic, EPR, and vibrational spectra of $(cyclamH_4)CuCl_6$ (cyclam = 1,4,8,11-tetraazacyclotetradecane) are reported and interpreted in terms of the elongated tetragonal geometry of the isolated $CuCl_6^{4-}$ ions present in this compound. Comparisons have been made with chlorocuprates having other geometries. It is inferred from the electronic spectrum that the axial chloride ligands have a small but significant effect on the energy levels of $(cyclamH_4)CuCl_6$, despite their long distance from the metal ion (317.5 pm), and this interaction leads to the near degeneracy of the d_{z^2} and $d_{xz,yz}$ orbitals in the $CuCl_6^{4-}$ complex. Angular overlap metal–ligand-bonding parameters have been derived and compared with those of other complexes with differing degrees of tetragonal distortion.

Introduction

Because chlorocuprates are comparatively simple and exhibit a wide range of stereochemistries, they have often been used to probe the ways in which various spectroscopic and bonding properties change as a function of geometric distortion.[1] Particular attention has been paid to the electronic, EPR, and vibrational spectra of the four-coordinate $CuCl_4^{2-}$ ion as this changes between a square-planar and a tetrahedral geometry.[2-7] The five-coordinate $CuCl_5^{3-}$ complex is unusual, since although the most stable configuration is apparently a square-based pyramid, vibronic coupling induces a dynamic equilibrium that produces a time-averaged trigonal-bipyramidal geometry.[8] Considerable interest has also been shown in the spectroscopic changes accompanying axial ligation of planar $CuCl_4^{2-}$ to produce a tetragonally elongated six-coordinate $CuCl_6^{4-}$ complex.[9-11] However, until now, the latter studies have involved compounds of the form $(cation)_2CuCl_4$, with axial coordination occurring by the linkage of neighboring complexes to form infinite polymers. Despite several attempts to produce compounds containing isolated $CuCl_6^{4-}$ groups,[12,13] it is only recently that this has been achieved in the compound $(cyclamH_4)CuCl_6$ (cyclam = 1,4,8,11-tetraazacyclotetradecane).[14] The present paper reports the spectral properties and bonding characteristics of this compound and compares these with the behavior of chlorocuprates having other stereochemistries.

Experimental Section

The preparation and characterization of $(cyclamH_4)CuCl_6$ has been described previously.[14] Infrared spectra were measured as polythene disks by using a Digilab FTS 20E Fourier transform spectrometer using a 6.25-μm beam splitter. Raman spectra were recorded with a Cary 82 spectrophotometer fitted with an argon laser using the 488-nm excitation line. A powdered sample pressed into a disk was used, with this being rotated in a spinning cell to minimize overheating. Electronic spectra of single crystals were measured upon a Cary 17 spectrophotometer using polarized light by a method described previously.[15,16] The crystals were cooled by using a Cryodyne Model 22C cryocooler. EPR spectra were recorded at room temperature by using a JEOL JES-FE X-band spectrometer.

Results and Discussion

Geometry of the $CuCl_6^{4-}$ Ion. The triclinic unit cell of $(cyclamH_4)CuCl_6$ contains a single formula unit.[14] The $CuCl_6^{4-}$ ion lies on an inversion center, with the elongated tetragonal stereochemistry so often observed for Cu(II) complexes. The in-plane bonds are almost equal (229.1 and 230.2 pm) and are much shorter than the axial bonds (317.5 pm), and the ClCuCl angles involving the in-plane ligands differ from 90° by less than a degree. The

* To whom correspondence should be addressed.

(1) Smith, D. W. *Coord. Chem. Rev.* **1976**, *21*, 93.
(2) Sherren, A. T.; Ferraro, J. R. *Inorg. Chim. Acta* **1977**, *22*, 43.
(3) Battaglia, L. P.; Bonamartini Corradi, A.; Marcotrigiano, G.; Menabue, L.; Pellacani, G. C. *Inorg. Chem.* **1979**, *18*, 148.
(4) Desjardins, S. R.; Penfield, K. W.; Cohen, S. L.; Musselman, R. L.; Solomon, E. I. *J. Am. Chem. Soc.* **1983**, *105*, 4590.
(5) Deeth, R. J.; Hitchman, M. A.; Lehmann, G.; Sachs, H. *Inorg. Chem.* **1984**, *23*, 1310.
(6) McDonald, R. G.; Riley, M. J.; Hitchman, M. A. *Inorg. Chem.* **1988**, *27*, 894.
(7) Bond, M. R.; Johnson, T. J.; Willett, R. D. *Can. J. Chem.* **1988**, *66*, 963 and references therein.
(8) Reinen, D.; Friebel, C. *Inorg. Chem.* **1984**, *23*, 791.
(9) Smith, D. W. *Inorg. Chim. Acta* **1977**, *22*, 107.
(10) Hitchman, M. A.; Cassidy, P. J. *Inorg. Chem.* **1978**, *17*, 1682.
(11) Deeth, R. J.; Gerloch, M. *Inorg. Chem.* **1985**, *24*, 1754.
(12) Larsen, K. P.; Hazell, R. G.; Toftlund, H.; Anderson, P. R.; Bisgard, P.; Edlund, K.; Eliasen, M.; Herskind, C.; Laursen, A.; Pedersen, P. M. *Acta Chem. Scand. A* **1975**, *29*, 499.
(13) Antolini, L.; Menabue, L.; Pellacani, G. C.; Saladini, M.; Marcotrigiano, G. *Inorg. Chim. Acta* **1982**, *58*, 193.
(14) Studer, M.; Riesen, A.; Kaden, Th. A. To be submitted for publication in *Helv. Chim. Acta*.
(15) McDonald, R. G.; Hitchman, M. A. *Inorg. Chem.* **1986**, *25*, 3273.
(16) Hitchman, M. A. *Transition Met. Chem. (N.Y.)* **1985**, *9*, 1.

0020-1669/89/1328-3996$01.50/0 © 1989 American Chemical Society